Embedding Quasicrystals in a Periodic Cell: Dynamics in Quasiperiodic Structures

Atahualpa S. Kraemer* and David P. Sanders†

Departamento de Física, Facultad de Ciencias, Universidad Nacional Autónoma de México, Ciudad Universitaria, México D.F. 04510, Mexico

(Received 31 May 2012; revised manuscript received 24 March 2013; published 18 September 2013)

We introduce a construction to ''periodize'' a quasiperiodic lattice of obstacles, i.e., embed it into a unit cell in a higher-dimensional space, reversing the projection method used to form quasilattices. This gives an algorithm for simulating dynamics, as well as a natural notion of uniform distribution, in quasiperiodic structures. It also shows the generic existence of *channels*, where particles travel without colliding, up to a critical obstacle radius, which we calculate for a Penrose tiling. As an application, we find superdiffusion in the presence of channels, and a subdiffusive regime when obstacles overlap.

DOI: 10.1103/PhysRevLett.111.125501 PACS numbers: 61.44.Br, 05.45.Pq, 05.60.Cd, 66.30.je

Quasicrystals are produced by cooling from a melt at a rate intermediate between that of periodic crystals (slow) and glasses (fast), and have a degree of order which is intermediate between the two, being neither periodic nor random [1–4]. Such structures have been found and applied in many different contexts, including liquid crystals [5], bilayer water [6], asteroids [7,8], magnetic systems [9], and photonics [10].

Transport properties of quasicrystalline materials are of particular interest for their production and for technological applications [11]. Diffusion has been extensively studied experimentally [12–14]; it is related to other transport properties, such as heat conductivity and electronic transport [12]. The measured thermopower in quasicrystals is due to electron diffusion [15], and diffusion plays a role in the formation of the equilibrium phase during high-temperature annealing [16].

Since quasicrystals are often perfect quasilattices [17], it is useful to study simple models in order to understand the effect of geometry on transport properties. A widely used billiard model for transport properties is the Lorentz gas (LG) [18], consisting of an array of fixed obstacles in $\mathbb{R}^n$, with freely moving particles undergoing elastic collisions with the obstacles.

The geometry in which the obstacles are arranged in a LG strongly influences its dynamical properties. LGs with a periodic geometry usually exhibit normal diffusion, i.e., asymptotic behavior $\langle \Delta x(t)^2 \rangle \sim t$ as $t \to \infty$ for the mean-squared displacement [19–23]; here, $\Delta x(t) := x(t) - x(0)$ is the displacement of a particle at time t, and $\langle \cdot \rangle$ denotes an average over uniform initial conditions. However, a key role is played by the presence of channels, i.e., empty regions through which particles may travel infinitely far without colliding: channels of the highest dimension, $n - 1$, give rise to weak superdiffusion of the form $\langle \Delta x(t)^2 \rangle \sim t \ln t$, with a logarithmic correction [23–27].

If the obstacles are placed randomly, but without overlap, normal diffusion is found [28]. When overlaps are allowed, there is a crossover from a subdiffusive regime, $\langle \Delta x(t)^2 \rangle \sim t^\alpha$ with $\alpha < 1$, to normal diffusion at long times; the slowdown of diffusion is due to the presence of large traps near the percolation threshold [29–33].

It is then natural to investigate dynamics, and in particular diffusive transport, for the intermediate case, a quasiperiodic LG, as suggested in Ref. [34] for a Penrose tiling. A random walk on this structure exhibits normal diffusion [35], suggesting that the same should occur in the billiard model [34]. We are not aware of previous numerical results in this direction, except in a nonphysical one-dimensional (1D) system [36], mainly due to the challenge of simulating quasiperiodic systems in the absence of periodic boundary conditions. Recently, the distribution of free paths in quasicrystals has been established in the so-called Boltzmann-Grad limit [37].

In this Letter, we introduce a construction to embed quasiperiodic structures into a periodic system of higher dimension, by reversing the projection method used to produce quasiperiodic lattices [38–40]. Our construction solves the principal difficulty with quasiperiodic systems, by reducing the system to a single periodic unit cell, and hence to a finite (compact) set, now in the higher-dimensional system; see also Ref. [37].

This has several implications. First, it provides a direct method for understanding and numerically simulating dynamics in quasiperiodic structures. Second, it gives a natural notion of uniform distribution (measure), and hence of averages, in quasiperiodic systems.

Motivated by the results cited above on periodic Lorentz gases, as well as by Ref. [34], where it was suggested that the absence of periodicity may prevent the occurrence of channels, and by Refs. [41,42], where it was shown experimentally and analytically that interplane and interline distances in certain perfect quasilattices are finite, we may ask when a quasiperiodic LG may contain channels. A third consequence of our construction is that in fact this occurs generically: when the obstacles of a quasiperiodic LG are sufficiently small, it does contain channels.

As an example, we apply our method to study diffusive properties of a particular 2D quasiperiodic LG, finding three regimes, including superdiffusion in the presence of channels, a subdiffusive regime when the obstacles overlap, and normal diffusion for intermediate geometries. We also find explicitly the critical obstacle radius at which channels are blocked in the quasiperiodic Penrose tiling.

Projection method.—The projection method [38,39,43] constructs a quasiperiodic lattice in a subspace E (including the origin) of a Euclidean space $\mathbb{R}^n$ by projecting vertices of a hypercubic lattice L, consisting of points with integer coordinates in $\mathbb{R}^n$, onto E [38–40]. We denote by m the dimension of E, with $m < n$, and by $E_\perp$ the orthogonal complement of E, of dimension $n - m$, such that $E \oplus E_\perp = \mathbb{R}^n$. In the following, we refer to orthogonal projections as "projections."

One version of the projection method [39] considers the Voronoi region of a lattice point p of L, i.e., a cube centered at p, projecting onto E exactly those p whose Voronoi regions intersect E; see Fig. 1(a). This gives a set $L_\parallel$ of points in E, which is a quasiperiodic lattice if E is *totally irrational* [39].

The Voronoi projection method produces the same quasilattice as the following canonical projection method [39]: consider a cube whose side length is the lattice spacing, centred at the origin, and project it onto the orthogonal subspace $E_\perp$, giving a set W. The lattice points in L which lie inside $W \times E$ are projected onto E; see Fig. 1(b).

Construction of embedding.—The quasiperiodic LG consists of balls of dimension m in E centred at each point of $L_\parallel$. We "reverse" the projection method to construct a billiard obstacle K inside a unit cube C of $\mathbb{R}^n$ with periodic boundary conditions, designed such that trajectories of the billiard dynamics in C with velocities *parallel* to E give trajectories of the quasiperiodic LG when the dynamics is "unfolded" to $\mathbb{R}^n$, by using periodic boundary conditions in one cell, but keeping track of which cell has been reached [44].

Consider free motion of a particle inside C whose velocity is constrained to move parallel to E. When the particle reaches a face of C, it jumps to the opposite face, due to the periodic boundary conditions, but maintains the same velocity. It then moves on a different "slice", $E_\mathbf{v} := E + \mathbf{v}$, parallel to E but translated by a vector $\mathbf{v} \in E_\perp$; see Fig. 2(a). In this way, the whole of the plane E is "wrapped" into one single unit cell C.

Since E is totally irrational, a trajectory emanating from a generic initial condition inside the cube C will fill C densely [45]; similarly, the collection of parallel slices $E_\mathbf{v}$ which are visited by a given trajectory also fill C densely [45].

C can now be thought of as representing *each* Voronoi cell in $\mathbb{R}^n$ which intersects E. The projection method then requires to project the origin onto each slice $E_\mathbf{v}$ intersecting C. We denote by W the set of such points; it is exactly the projected set used in the canonical projection method. W is a subset of full dimension inside $E_\perp$, which can be constructed by projecting the vertices of C onto $E_\perp$ and taking the convex hull.

We now project onto $E_\perp$ not just a single point at the origin, but the whole billiard obstacle B in E, an m-dimensional ball of radius r centered at the origin. The result is a new set $P := W \times B$ of full dimension n. However, some parts of P fall outside C, as shown in Fig. 2(a). We must thus *periodize* P via the periodic boundary conditions, giving a set K, which is the final result of the construction, a billiard obstacle inside C.

To simulate the quasiperiodic billiard in the m-dimensional space E, we run billiard dynamics inside the n-dimensional cube C, imposing elastic collisions with the billiard obstacle K. The particles have initial velocities parallel to E; since the boundary of K is cylindrical, with axis perpendicular to E, collisions of the particles with K do not (in principle) affect this property, so that they remain parallel to E during the dynamics. (In practice, in

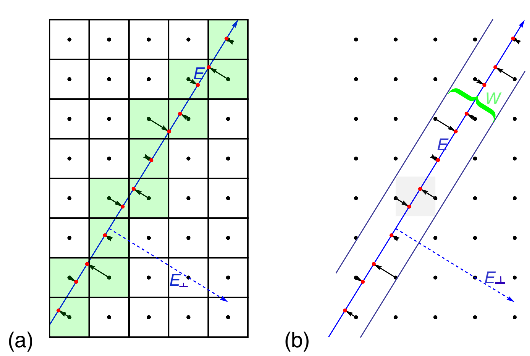

FIG. 1 (color online). Two versions of the projection method: (a) Voronoi regions, shown as shaded (green) boxes; arrows show lattice points in L that are projected onto the line E. (b) Canonical version, projecting lattice points inside a strip.

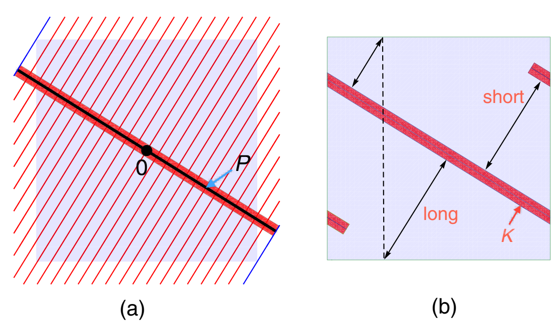

FIG. 2 (color online). Embedding a 1D quasiperiodic lattice into a 2D periodic billiard. (a) Construction of the set P by projection and "thickening." Parallel diagonal lines (red online) show "slices" $E_\mathbf{v}$. (b) The billiard obstacle K, after periodizing P, made of three oblique (red) bars. Short and long paths for the billiard dynamics are shown.

a numerical simulation, it is desirable to project the velocities onto E at intervals.) When the resulting billiard trajectory is unfolded to $\mathbb{R}^n$, it gives exactly a billiard trajectory in the quasiperiodic LG.

Uniform distribution.—Our construction provides a natural way to define a uniform distribution (measure) on the phase space of a quasiperiodic system: particle positions are uniform in the cube C outside the billiard obstacle K, and velocities have unit speed and uniform directions parallel to E. Averages are then taken with respect to this uniform distribution. We conjecture that the dynamics in a quasiperiodic LG is ergodic; i.e., from almost any (accessible) starting point, the trajectory fills uniformly the accessible phase space.

The simplest example is a 1D quasiperiodic billiard with $n = 2$ and $m = 1$, so that C is a square, E is a straight line with irrational slope α, and B is a line segment of length r. The set K then consists of three thickened line segments with slope $-1/\alpha$; see Fig. 2(b). Since K divides the square completely into two parts, there is, as expected, no diffusion in this case: any given trajectory remains confined, bouncing between two neighboring obstacles. However, our construction easily allows us to calculate, for example, the probabilities of long and short paths from uniform initial conditions, in terms of the sizes of the respective areas [see Fig. 2(b)].

2D quasiperiodic Lorentz gas.—A nontrivial example in which the construction may be visualized is a 2D quasiperiodic LG formed by projecting a 3D simple cubic lattice, with cubic unit cell C, onto a totally irrational 2D plane E, with B being a disc of radius r and W a 1D line perpendicular to E; the resulting 3D periodic billiard is shown in Fig. 3. The obstacle K consists of three segments

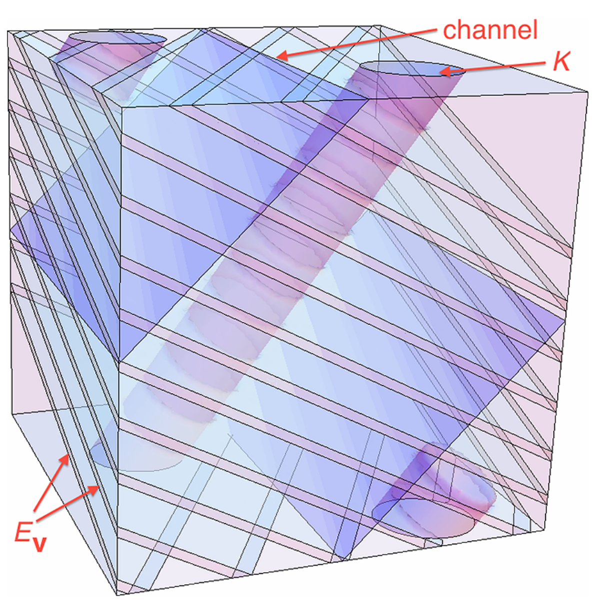

FIG. 3 (color online). 2D quasiperiodic LG embedded in a 3D cube, with notation as in the text.

of a cylinder, and the two parts of the cylinder which arise by periodizing P are capped by planes E_v passing through vertices of C.

Channels.—This 2D LG (Fig. 3) provides an example in which the occurrence of channels in quasiperiodic LGs may be visualised, thus providing intuition for the general case, as follows.

The axis W of the cylinder K intersects two of the cube's faces. Suppose that the radius r of the obstacle B, and hence of the cylinder K, is small enough that there is (at least) one face of the cube which is not intersected by any of the three cylindrical pieces of K. Then in the 3D billiard with arbitrary velocities (not restricted to be parallel to E) there is a planar channel Π [23] lying along any such face.

Now restricting particle velocities to be parallel to E, we see that each planar channel Π in the 3D periodic billiard induces a rectangular channel in the 2D quasiperiodic LG, given by the intersection of E with Π. As in the periodic LG [24,25], additional channels may appear as the radius decreases; for example, Fig. 3 shows an additional planar channel at an angle $\pi/4$.

This generalizes to quasiperiodic LGs in $m > 2$ dimensions with $(m-1)$-dimensional principal horizons [46]. Thus our construction shows the generic occurrence of channels in quasiperiodic Lorentz gases when the obstacles have sufficiently small radius.

As r increases, the channels are blocked one by one, as the billiard obstacles expand sufficiently to intersect the planes defining the channels. When the billiard obstacles are large enough to cross the faces of the cube, their periodic images must also be taken into account as additional obstacles in the simulations; for this reason, the algorithm is most efficient when the obstacles are small, which is the most difficult case to treat using standard methods.

Diffusive properties.—Our construction immediately gives a direct simulation method for quasiperiodic billiard dynamics. As an example, we numerically study diffusive properties of the 2D quasiperiodic LG projected from three dimensions: We place 10^6 (noninteracting) particles with uniform positions in the 3D unit cube C, and unit-speed velocities with uniform directions parallel to the plane E with unit normal vector $[1/(\phi+2), \phi/(\phi+2), \phi/(\sqrt{\phi+2})]$, where $\phi := (1+\sqrt{5})/2$.

Figure 4 plots $\langle \Delta x(t)^2 \rangle / t$, to emphasize deviations from normal diffusion [47], for different radii r of the billiard obstacles. We see that for small radii, this quantity increases logarithmically in time, indicating (weak) superdiffusion $\langle \Delta x(t)^2 \rangle \sim t \ln t$, as in the periodic case, corresponding to the presence of channels in the quasiperiodic LG.

However, the convergence to this limiting regime is very slow. We interpret this as being due to regions adjacent to the infinite channels in which free paths are unbounded, but not infinite ("locally finite"); this phenomenon does not occur in periodic models. For short times, the effective

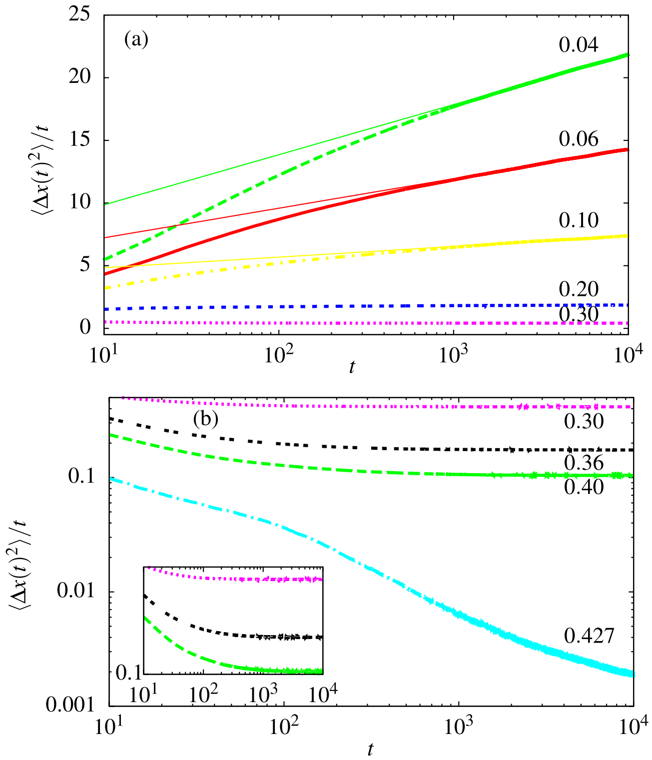

FIG. 4 (color online). $\langle \Delta x(t)^2 \rangle / t$ as a function of t for different radii r (labelled), for the quasiperiodic LG in two dimensions projected from three dimensions. (a) Semilogarithmic scale. The thin solid lines show fits of the form $\langle x(t)^2 \rangle = C(r) t \ln t + D(r) t$. (b) Logarithmic scale; the inset emphasizes curvature.

width of the channel is thus larger, giving a decreasing effective superdiffusion coefficient as time increases, and hence the curvature visible in Fig. 4. These regions are always associated with channels, except exactly at the critical radius $r = r_c$, when all channels are blocked, but free paths are still unbounded, as we will discuss elsewhere; we find normal diffusion in this case [46].

As the obstacle radius, r, increases, the geometry of the quasiperiodic LG, and hence the diffusive behavior, undergoes qualitative changes. At $r \simeq 0.26$, the obstacles begin to overlap [46]. In this model, this overlap occurs *before* the last planar channel is blocked, so that we expect superdiffusion; however, we are unable to detect this numerically, and the diffusion appears normal already for $r = 0.20$ (with a channel, but not overlapping). In the Penrose LG, on the contrary, all channels are blocked before any obstacles overlap.

At the critical radius $r_c \simeq 0.3$, all channels are blocked. For $r > r_c$, we observe an initial subdiffusive regime, with a crossover to normal diffusion at long times, as in the random LG; see Fig. 4(b). Finally, there is a radius $r \simeq 0.428$ at which particles become confined in bounded regions. Note that these values of r can be calculated analytically, but the results are complicated functions of the geometrical parameters.

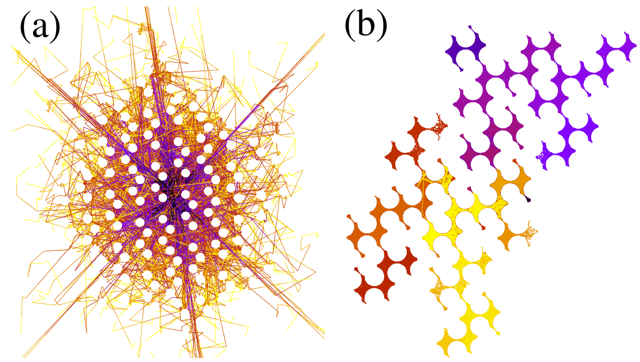

FIG. 5 (color online). Representative trajectories of 2D quasiperiodic LG projected from three dimensions. The gray (color) scale indicates time. Blank, circular regions correspond to the billiard obstacles, whose positions are identical in the two subfigures. (a) $r = 0.18$; several initial conditions. (b) $r = 0.425$; single initial condition.

Figure 5(a) shows representative trajectories for $r = 0.18$, highlighting the channels within the quasiperiodic LG. There are channels in three directions, corresponding to those in Fig. 3—two along two perpendicular, vertical faces of the cube, and one at an angle of $\pi/4$. Figure 5(b) shows a single trajectory for large r, close to the percolation threshold at which diffusion ceases. Narrow bottlenecks between cavities of different sizes are visible, which we interpret as the origin of the observed slow diffusive behavior.

Penrose Lorentz gas.—Our construction may also be carried out for more realistic models, such as a Penrose LG, formed by placing discs at each vertex of a Penrose tiling [34]. This structure is obtained by projecting a 5D lattice onto a 2D subspace E [38,39], so that P is a 5D cylinder, the product of a 3D polytope W [38] with a 2D ball.

Our results show that the Penrose LG must have channels for obstacle radius r less than a critical value r_c. To calculate r_c, we must find when at least one 4D (hyper-) face of the 5D hypercube C is not touched by K. Thus, for each face of C, we find the minimum distance (in the direction of E) to all vertices p_i of W. The maximum over all faces then seems to be enough to calculate r_c, or at least a lower bound [46]. For the Penrose tiling, the symmetry implies that many of these distances are equal, and we obtain $r_c = L/(2\tau^2)$, where $\tau = (1 + \sqrt{5})/2$ and L is the side length of the rhombi forming the tiling, which we have confirmed numerically [46].

In summary, we have introduced a construction to embed quasiperiodic lattices into a unit cell in a higher-dimensional space, which shows that quasiperiodic Lorentz gases generically have channels for small obstacle radii, and which provides a direct simulation method for dynamics in quasiperiodic structures. These systems exhibit a range of diffusive properties, including super- and subdiffusion, depending on the geometry. We expect that our construction can be profitably applied to further phenomena in quasiperiodic systems.

The authors thank C. Dettmann, H. Spohn, and D. Szász for discussions. Financial support is acknowledged from CONACYT for ASK's doctoral studentship, and from the SEP-CONACYT Grant No. CB-101246.

Note added in proof.—During revision of the proofs, the authors found previous results which are apparently related, e.g., [48]. However, in those references, *starting* from *any* higher-dimensional periodic system, a quasilattice of points is obtained by a cut procedure, and structural properties are studied; whereas we *construct specific* higher-dimensional billiard models in order to study *dynamics*.

*ata.kraemer@gmail.com
†dpsanders@ciencias.unam.mx

[1] D. Shechtman, I. Blech, D. Gratias, and J. W. Cahn, Phys. Rev. Lett. **53**, 1951 (1984).
[2] J. Holzer and K.F. Kelton, in *Quasicrystals and Incommensurate Structures in Condensed Matter: Third International Meeting*, edited by M.J. Yacaman and M. Torres (North Holland, Amsterdam, 1993), p. 103.
[3] A. Haji-Akbari, M. Engel, A.S. Keys, X. Zheng, R.G. Petschek, P. Palffy-Muhoray, and S.C. Glotzer, Nature (London) **462**, 773 (2009).
[4] B. Chakraborty, Phys. Rev. B **38**, 345 (1988).
[5] X. Zeng, G. Ungar, Y. Liu, V. Percec, A.E. Dulcey, and J.K. Hobbs, Nature (London) **428**, 157 (2004).
[6] J.C. Johnston, N. Kastelowitz, and V. Molinero, J. Chem. Phys. **133**, 154516 (2010).
[7] L. Bindi, P.J. Steinhardt, N. Yao, and P.J. Lu, Science **324**, 1306 (2009).
[8] L. Bindi, J.M. Eiler, Y. Guan, L.S. Hollister, G. MacPherson, P.J. Steinhardt, and N. Yao, Proc. Natl. Acad. Sci. U.S.A. **109**, 1396 (2012).
[9] K. Deguchi, S. Matsukawa, N.K. Sato, T. Hattori, K. Ishida, H. Takakura, and T. Ishimasa, Nat. Mater. **11**, 1013 (2012).
[10] S.M. Thon, W.T.M. Irvine, D. Kleckner, and D. Bouwmeester, Phys. Rev. Lett. **104**, 243901 (2010).
[11] F. Samavat, M. Gladys, C. Jenks, T. Lograsso, B. King, and D. O'Connor, Surf. Sci. **601**, 5678 (2007).
[12] L. Guidoni, B. Dépret, A. di Stefano, and P. Verkerk, Phys. Rev. A **60**, R4233 (1999).
[13] T. Zumkley, H. Mehrer, K. Freitag, M. Wollgarten, N. Tamura, and K. Urban, Phys. Rev. B **54**, R6815 (1996).
[14] H. Mehrer and R. Galler, J. Alloys Compd. **342**, 296 (2002).
[15] K. Giannò, A. Sologubenko, M. Chernikov, H. Ott, I. Fisher, and P. Canfield, Mater. Sci. Eng., A **294–296**, 715 (2000).
[16] S. Hocker, F. Gähler, and P. Brommer, Philos. Mag. **86**, 1051 (2006).
[17] Z. Papadopolos, J. Phys. Conf. Ser. **226**, 012003 (2010).
[18] H.A. Lorentz, Proc. R. Acad. Amst. **7**, 438 (1905).
[19] C. Bruin, Phys. Rev. Lett. **29**, 1670 (1972).
[20] B. Moran and W.G. Hoover, J. Stat. Phys. **48**, 709 (1987).
[21] L.A. Bunimovich and Y.G. Sinai, Commun. Math. Phys. **78**, 479 (1981).
[22] N.I. Chernov, G.L. Eyink, J.L. Lebowitz, and Y.G. Sinai, Commun. Math. Phys. **154**, 569 (1993).
[23] D.P. Sanders, Phys. Rev. E **78**, 060101 (2008).
[24] P.M. Bleher, J. Stat. Phys. **66**, 315 (1992).
[25] D. Szász and T. Varjú, J. Stat. Phys. **129**, 59 (2007).
[26] C.P. Dettmann, J. Stat. Phys. **146**, 181 (2012).
[27] D.I. Dolgopyat and N.I. Chernov, Russ. Math. Surv. **64**, 651 (2009).
[28] A.B. Adib, Phys. Rev. E **77**, 021118 (2008).
[29] J. Machta and S.M. Moore, Phys. Rev. A **32**, 3164 (1985).
[30] T. Franosch, M. Spanner, T. Bauer, G.E. Schröder-Turk, and F. Höfling, J. Non-Cryst. Solids **357**, 472 (2011).
[31] F. Höfling, T. Franosch, and E. Frey, Phys. Rev. Lett. **96**, 165901 (2006).
[32] W. Götze, E. Leutheusser, and S. Yip, Phys. Rev. A **23**, 2634 (1981).
[33] W. Götze, E. Leutheusser, and S. Yip, Phys. Rev. A **25**, 533 (1982).
[34] D. Szász, Nonlinearity **21**, T187 (2008).
[35] A. Telcs, J. Stat. Phys. **141**, 661 (2010).
[36] B. Wennberg, J. Stat. Phys. **147**, 981 (2012).
[37] J. Marklof and A. Strömbergsson, arXiv:1304.2044.
[38] N. de Bruijn, Ned. Akad. Wet. Proc. Ser. A **43**, 39 (1981).
[39] M. Senechal, *Quasicrystals and Geometry* (Cambridge University Press, Cambridge, England, 1995).
[40] P. Kramer and R. Neri, Acta Crystallogr. Sect. A **40**, 580 (1984).
[41] Z. Papadopolos, P. Pleasants, G. Kasner, V. Fournée, C.J. Jenks, J. Ledieu, and R. McGrath, Phys. Rev. B **69**, 224201 (2004).
[42] Z. Papadopolos and G. Kasner, Phys. Rev. B **72**, 094206 (2005).
[43] J.L. Aragón, D. Romeu, L. Beltrán, and A. Gómez, Acta Crystallogr. Sect. A **53**, 772 (1997).
[44] N. Chernov and R. Markarian, *Chaotic Billiards* (American Mathematical Society, Providence, RI, 2006).
[45] A. Katok and B. Hasselblatt, *Introduction to the Modern Theory of Dynamical Systems* (Cambridge University Press, Cambridge, England, 1997).
[46] A.S. Kraemer and D.P. Sanders (to be published).
[47] D.P. Sanders and H. Larralde Phys. Rev. E **73**, 026205 (2006).
[48] C. Janot, *Quasicrystals: A Primer* (Oxford University Press, Oxford, UK, 1994), 2nd ed., and references therein.